ISBN: 978-3-95450-232-5 ISSN: 2673-7000 doi:10.18429/JACoW-NAPAC2022-WEPA10

DETERMINATION OF LCLS-II GUN-2 PROTOTYPE DIMENSIONS*

L. Xiao†, C. Adolphsen, E. Jongewaard, X. Liu, F. Zhou
SLAC National Accelerator Laboratory, Menlo Park, CA, USA

Abstract

The LCLS-II spare gun (Gun-2) design is largely based on the existing LCLS-II gun (Gun-1), in which there is significant captured dark current (DC) that originates on the high field copper surface near the cathode plug gap opening. To help suppress DC, the Gun-2 cathode and anode noses and the cathode plug opening are elliptically shaped to minimize the peak surface field for a given cathode gradient. In addition, stainless steel (SS) cathode and anode nose inserts are used in Gun-2 to further reduce dark current as SS has a lower potential for field emission. The cavity full 3D RF simulations were performed including vacuum slots, input couplers and probe and view ports. The thermal and structural analyses were done to investigate the effects of atmospheric pressure and RF heating. The multi-physics simulation results provided the information needed to determine the Gun-2 prototype dimensions. The Gun-2 cathode-to-anode gap distance will be made 1 mm longer than the nominal gap with the expectation that less than 1 mm will be machined off to meet the target frequency. In this paper, the Gun-2 frequency correction calculations are presented, and the cathode-to-anode gap determination is discussed.

2D CAVITY DESIGN

The LCLS-II spare gun (Gun-2) design is largely based on the existing LCLS-II gun (Gun-1), which was designed and built at LBNL. To help suppress dark current, the Gun-2 cathode and anode nose and the cathode plug opening are elliptically shaped to minimize the peak surface field for a given cathode gradient by LBNL and further optimized by SLAC [1]. The Gun-1 and Gun-2 RF parameters are listed in Table 1. The peak surface electric field in Gun-2 is lower by 10%.

Table 1: RF Parameters for a 750 keV Energy Gain

2D Cavity	Gun-1	Gun-2
Frequency (MHz)	186.850	186.018
Accelerating gap (mm)	40	40
Quality factor Q_0	~3.12x10^4	~3.12x10^4
Shunt impedance R/Q (Ω)	202	208
Cathode E_c(MV/m)	19.5	19.8
Peak surface E_{peak} (MV/m)	24.4	21.6
RF power loss (kW)	87	85

3D CAVITY RF SIMULATIONS

There are two sets of identical loop fundamental power couplers (FPC) in Gun-2, which are of the same design as used in Gun-1. The Gun-2 3D RF simulations were performed using the SLAC parallel finite-element electromagnetics code suite ACE3P [2]. The 3D gun cavity is shown in Fig. 1 including vacuum slots, input couplers and probe and view ports. The angles of the FPC loop antennas can be adjusted to achieve critical external coupling Q_{ext}, that is Q_{ext} = Q_o with fixed antenna intrusions of 4.47 mm. The resonant mode electric and magnetic fields for the critical coupling are shown in Fig. 2 for a loop angle of 70°. The frequency is 226 kHz lower due to the 3D features. Removing the antennas and blanking off the FPC ports, the cavity frequency reduces by 40 kHz. Taking off the cathode plug increases the cavity frequency by 6 kHz.

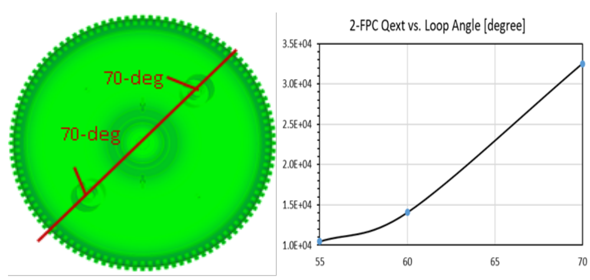

Figure 1: The Gun-2 3D geometry showing the couplers and their loop orientations at the critical coupling (left) and Q_{ext} versus the loop angle in degrees (right).

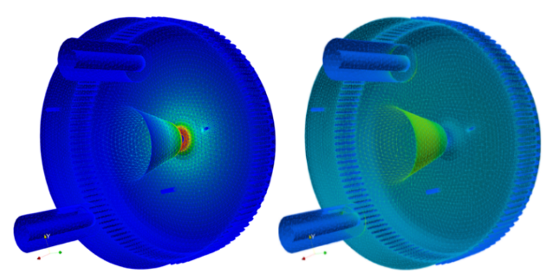

Figure 2: The complex electric (left) and magnetic (right) fields in the Gun-2 3D geometry when Q_{ext} = Q_o.

CAVITY THERMAL AND STRUCTURAL ANALYSIS

Atmospheric Pressure

The Gun-2 engineering design tries to maintain the overall dimensions of Gun-1 so it will be plug compatible with Gun-1. In particular, the dimensions DIM-A, DIM-B and DIM-C shown for Gun-1 in Fig. 3 are similar for Gun-2. However, there are some minor differences due to the improvements that were made for Gun-2.

A quarter of Gun-1 and Gun-2 solid models without the FPCs and small ports shown in Fig. 4 are simulated for thermal and structural analysis.

* Work supported by US DOE under contract AC02-76SF00515.
† liling@slac.stanford.edu

ISBN: 978-3-95450-232-5 ISSN: 2673-7000 doi:10.18429/JACoW-NAPAC2022-WEPA10

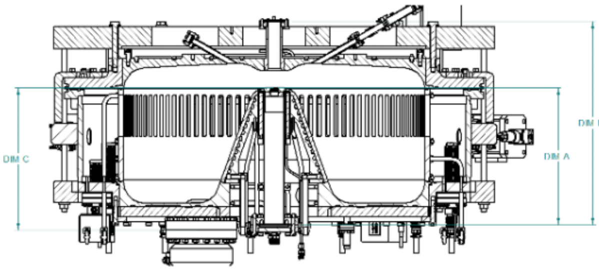

Figure 3: Gun-1 cross section.

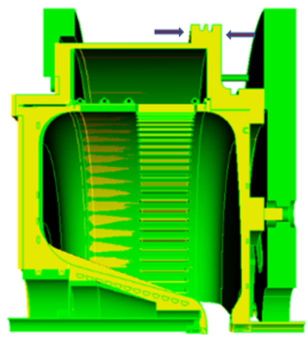

Figure 4: An overlay of the Gun-1 (yellow) and Gun-2 (green) solid models.

When the cavity is brought under vacuum, there is a $1.0\text{x}10^5$ Pa of atmospheric pressure loading outside the cavity enclosure to cause the cavity deformed. The clamps around the thin weld joint on the outer SS vacuum wall are not included in the simulation models. We force the two sides of the joint fixed at z-direction in an attempt account for the clamping force in the structural simulations. The two symmetry planes are symmetric constraint. The atmospheric pressure reduces the accelerating gap as shown in Fig. 5, and thus causes a decrease in the cavity frequency.

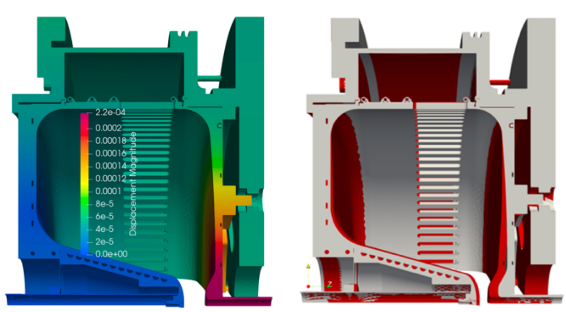

Figure 5: Gun-2 displacement amplitude (left) and geometries (right) without (grey) and with (red) atmospheric pressure. The geometry deformation is scaled 100 times large for visualizing.

The displacements due to the atmospheric pressure loading result in a 136 and 140 kHz frequency reduction in Gun-1 and Gun-2, respectively. The simulations suggested that Gun-1 and Gun-2 have similar structural support, which is desired.

Combining the frequency increasing of 56 kHz from air permittivity to vacuum, the simulated cavity frequency changes due to pump down are 80 and 84 kHz respectively compared to the Gun-1 measurement of 180 kHz. The simulation solid models are stiffener than the actual cases, and cause ~100 kHz less frequency detuning than the actual. Obtaining an accurate estimate of detuning in this case is difficult. There are several bolted or clamped connections on the cavity jacket that do not flex in the way that a solid connection would, which is how they are modeled in the simulations. Therefore, the Gun-1 measured frequency change of 180 kHz due to pump down is used to determine the Gun-2 final prototype dimensions.

RF Heat Load

LCLS-II Gun-2 anode plate flow rate is desired to be adjusted in the range of 2.0 to 4 gpm. The temperature profiles in Gun-2 with a 2.3 and 4 gpm anode flow rates for a cathode gradient of 20 MV/m are shown in Fig. 6. In the thermal simulations, the room temperature of 25 ^{0}C and the surrounding air convective coefficient of 10 W/m^2.K are assumed. One can see that the largest temperature rises occur on the anode nose for the lower anode flow rate and shift to the vacuum slot openings for the higher flow rate. The temperature on the anode nose is about 4 ^{0}C higher due to the SS insert in Gun-2 than Gun-1.

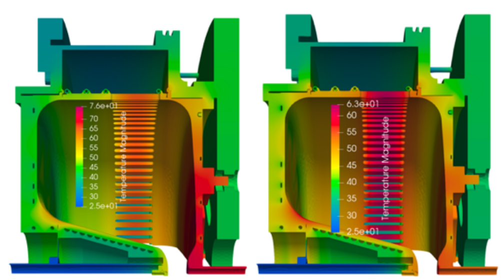

Figure 6: The temperature profiles with a 2.3 (left) and a 4.0 (right) gpm anode flow rates in Gun-2 solid model for a cathode gradient of 20 MV/m.

The detuning caused from the RF heating is mainly due to the outward bowing of the anode plate as it heats up more on the interior side than the exterior side where the cooling channels are located. The RF heating increases the accelerating gap, and thus causes an increase in the cavity frequency. The Gun-2 deformed cavities with different anode flow rates are shown in Fig. 7.

The RF detuning in Gun-1 and Gun-2 from the simulations are summarized in Table 2. The frequency increasing due to the RF heating for Gun-2 yields values about 20 kHz lower than Gun-1 for a cathode gradient of 20 MV/m, which the power loss is 91.5 and 86.7 kW in Gun-1 and Gun-2, respectively. Less 7 kW power loss in Gun-2 than Gun-1 results in about 17 kHz less rf frequency detuning based on the Gun-1 measurements. The simulations show that the flow rate changing from 2.3 to 4.0 gpm can reduce the cavity frequency about 70 kHz. In actual case, changing flow rate from 2.3 to 2.8 gpm can reduce the Gun-1cavity frequency by 70 kHz based on the measurements.

ISBN: 978-3-95450-232-5 ISSN: 2673-7000 doi:10.18429/JACoW-NAPAC2022-WEPA10

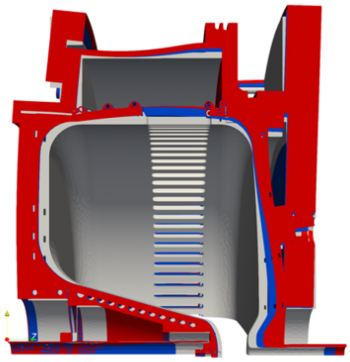

Figure 7: The deformed Gun-2 cavities with a 2.3 (red) and a 4.0 (blue) gpm anode flow rates for a cathode gradient of 20 MV/m and undeformed Gun-2 cavity (grey). The geometry deformations are scaled 100 times large for visualizing.

Table 2: Simulated RF Detuning for Ec=20 MV/m

Solid model	Gun-1	Gun-2
2.3 gpm	150 kHz	130 kHz
4.0 gpm	78 kHz	59 kHz

The simulation solid models are stiffener than the actual as mentioned before. The simulated RF detuning is ~100 kHz lower than the actual. In addition, there are some other RF detuning uncertainties such as the water temperature profile along the cooling channels (an estimated average temperature is assumed instead), the accurate heat transfer coefficients (*h*) on the cooling channels walls, and the actual air circulate condition during the gun operation. Therefore, the Gun-1 measured RF detuning is used to determine the Gun-2 final prototype dimensions.

FINAL PROTOTYPE DIMENSIONS

Moving the anode plate relative to the cathode section changes both the cavity frequency and field in the gap region, and provisions will be made to allow small gap changes during fabrication to fine tune the gun frequency before the anode plate is clamped to the cathode section. The cavity frequency sensitivity to the gap length is 541 kHz/mm. For this purpose, the cathode section will be made 1 mm longer than nominal with the expectation that less than 1 mm will be machined off to meet an intermediate target frequency.

Gun-2 is designed to work in push mode only with a 19 MV/m cathode gradient, 2.8 gpm anode flow rate and 2 kN per tuner push force. The frequency accounting connecting the 2D model frequency to the target machining frequency to the nominal operating frequency is summarized in Table 3. The Gun-2 final prototype accelerating gap would be 40.13mm. We expect that uncounted frequency error is less than 50 kHz. Changing the water flow rate in the anode plate from 2.3 to 4.0 gpm can accommodate +/- 70 kHz frequency error. Changing the tuner push force from zero to 4 kN can cover +/- 60 kHz as well. Moreover, 5% of the gradient variation can offset another +/- 25 kHz. During the Gun-2 operation, it is expected that +/- 150 kHz tuning range can be achieved.

Table 3: Frequency Corrections

Conditions	Relative dF (kHz)	Absolute F (MHz)
Operation		**185.714**
2kN push force	-60	
RF on	180	
Install cathode plug	-6	
Turn on LCW (30^0C)	-33	
Pump down	-180	
Add antennas	40	
		185.773
Machine off 0.87 mm, gap=40.13mm	-470	
Built 41mm gap	541	
Fill cavity with air	-56	
Remove cathode plug	6	
Add 3D features but w/o antenna	-266	
2D design. er = 1		**186.018**

ACKNOWLEDGEMENTS

The research used resources of the National Energy Research Scientific Computing (NERSC) Center, which is supported by the Office of Science of the U.S. Department of Energy under Contract No. DE-AC02-05CH11231.

REFERENCES

[1] L. Xiao *et al.*, "Spare Gun Multi-Physics Analysis for LCLS-II", in *Proc. 12th Int. Particle Accelerator Conf. (IPAC'21)*, Campinas, Brazil, May 2021, pp. 1688-1691. doi:10.18429/JACoW-IPAC2021-TUPAB127
[2] ACE3P code suite. https://conf.slac.stanford.edu/cw18/